International Journal of Mass Spectrometry and Ion Processes, 65 (1985) 169–180
Elsevier Science Publishers B.V., Amsterdam – Printed in The Netherlands

A STUDY OF THE METASTABLE FRAGMENTATION OF IONS PRODUCED BY ^{252}Cf FISSION FRAGMENT BOMBARDMENT OF BOVINE INSULIN

B.T. CHAIT and F.H. FIELD

Rockefeller University, New York, NY 10021 (U.S.A.)

(Received 21 November 1984)

ABSTRACT

A time-of-flight mass spectrometric study of the metastable decomposition of ions produced by ^{252}Cf fission fragment bombardment of bovine insulin is presented. The positive secondary ion insulin species investigated include the protonated molecular ion, the doubly charged quasi-molecular ion, the dimer ion, intact A- and B-chain fragment ions, and ions constituting the intense continuum which underlies the discrete peaks. A high proportion of secondary ions which enter the flight tube are observed subsequently to undergo unimolecular fragmentation during flight. Investigation of the temporal distribution of the flight-tube fragmentation indicate that the decays are heavily weighted to favor early times, i.e. high rate constants.

INTRODUCTION

The bombardment of surface organic molecules in the condensed phase by high energy fission fragments gives rise to a significant yield of secondary quasi-molecular (QM) ions, even for very polar and/or high molecular weight compounds [1–4]. At the same time, extensive prompt [1,3,5–8] and metastable fragmentation [6,7,9] is observed, indicating that a large proportion of the bombarded species become highly excited during the desorption and ionization processes. The fragmentation studies cited were made on a series of organic compounds with molecular weights less than 1000 u.

In the present work, our earlier investigation of the metastable decomposition of organic ions formed by fission fragment bombardment is extended to a considerably higher molecular weight compound, i.e. the polypeptide hormone bovine insulin with a monoisotopic molecular weight of 5729.6 (Fig. 1). Metastable fragmentation measurements are presented for the decay of the $(M + H)^+$ ion, the doubly charged QM ion, the dimer ion, intact A- and B-chain fragment ions, and ions constituting the intense continuum observed in the positive fission fragment-induced mass spectrum.

0168-1176/85/$03.30

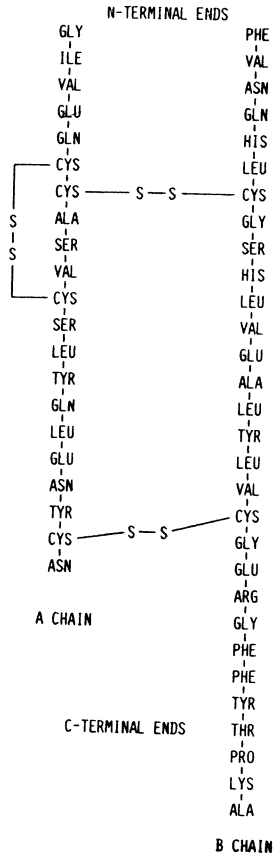

Fig. 1. Structure of bovine insulin.

Time-of-flight mass spectra of bovine insulin have previously been observed by the group at Uppsala using 90 MeV ^{127}I accelerator produced ions [10] and ^{252}Cf fission fragments [4,11]. Fast atom bombardment mass spectra of insulins have also been obtained using double focussing deflection mass spectrometers [12–16]. In one of these studies [16], the gas phase decompositions of the $(M + H)^+$ and $(M - H)^-$ ions of bovine insulin were measured. The findings of the present investigation are related to these earlier studies.

EXPERIMENTAL

The mass spectral measurements were made with the time-of-flight fission fragment ionization mass spectrometer built in this laboratory and described previously [3], A schematic drawing of the apparatus is given in Fig. 2. It contains three grids positioned close to the ion detector, the primary purpose

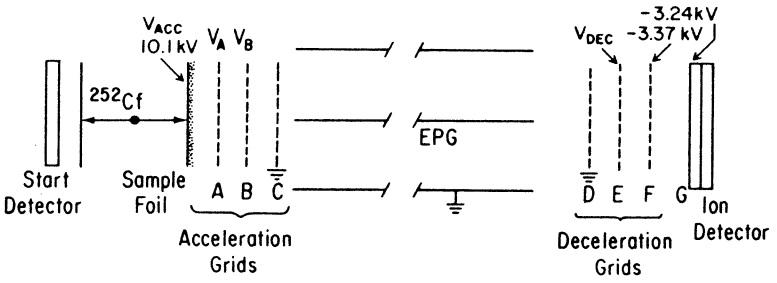

Fig. 2. Fission fragment ionization mass spectrometer, EPG is the electrostatic particle guide. Intergrid distances: $d_{foil-A} = 3.5$ mm, $d_{A-B} = 6.4$ mm, $d_{B-C} = 6.4$ mm, $d_{D-E} = 8.7$ mm, $d_{E-F} = 11.9$ mm and $d_{F-G} = 6.3$ mm.

of which is to provide a retarding potential for the study of fragmentation reactions occurring in the 3 m flight tube of the mass spectrometer [9]. It also contains three grids in the ion acceleration region. These enable measurements of rates of ion fragmentations in the acceleration region to be made as described in ref. 7.

The instrument also incorporates an electrostatic particle guide (EPG) [17] to enhance the transport of ions through the 3 m long flight tube. The EPG does not enhance the transport of neutral fragments, which are thus strongly discriminated against in the present instrument.

Samples of bovine insulin were obtained from the Sigma Chemical Co., St. Louis, MO. Following the Uppsala group [4,10], initial studies were performed with samples dissolved in neat trifluoroacetic acid (0.5 g l^{-1}) and electrosprayed [18] to a thickness of 20–40 μg on to an aluminized polyester foil with an area of 1 cm^2. This method of sample preparation produced a heterogenous mixture of compounds containing up to three trifluoroacetyl esters of insulin. Thus, for all the work described here, the sample was dissolved in and electrosprayed from glacial acetic acid, which yielded no significant ester formation. The fission fragment flux through the sample foil was 2000 fission fragments s^{-1} and run times typically ranged between 1 and 2 h.

The ion acceleration voltage applied to the sample foil was 10.1 kV. To increase the detection efficiency for high molecular weight species, the front face of the microchannel plate ion detector (G in Fig. 2) was coated by vacuum evaporation with a 500 Å thick layer of CsI and an additional 3.4 kV of post-acceleration was applied just prior to ion detection. In addition, a grid (F in Fig. 2) with a potential 130 V more negative than the front face of the detector was positioned 6.3 mm from the detector. This potential causes secondary electrons ejected from the front face of the microchannel plate to be reflected back into the plate and detected.

RESULTS AND DISCUSSIONS

The time-of-flight spectrum of bovine insulin with no metastable rejection is shown in Fig. 3. This spectrum was taken with the potentials on grids A, B, and E (Fig. 2) set to 0 V. Under these conditions, ions formed close to the sample foil, which survive further fragmentation until they are fully accelerated but which subsequently undergo metastable fragmentation in the field-free flight tube, contribute to the same peaks in the spectrum as do their precursor ions [9,19]. Such a time-of-flight spectrum thus provides a "snapshot" of the distribution of ions after a time equal to that required for full acceleration of the precursor species, e.g. 100 ns for a m/z 400 fragment and 380 ns for the $(M + H)^+$ ion from bovine insulin at m/z 5734 (isotopically averaged value). The primary effect of flight-tube metastable species on the spectrum is to broaden the peaks through the release of internal energy of excitation as translational energy of the fragments.

The spectrum given in Fig. 3 corresponds closely with that previously obtained by the Uppsala group [4,11]. The major ion peaks observed above m/z 2200 are listed in Table 1. The estimated errors on the measured masses include as their main components (a) calibration errors arising from the extrapolation from the calibration peaks at m/z 1 and 23 and (b) errors arising from the post-acceleration of ions which have undergone fragmentation in the flight tube. This latter error tends to give measured masses lower than the authentic values. The dominant high mass peak observed at m/z 5733.7 ± 2.0 corresponds, within the error of the determination, to the protonated molecular ion of bovine insulin. The other high mass ions

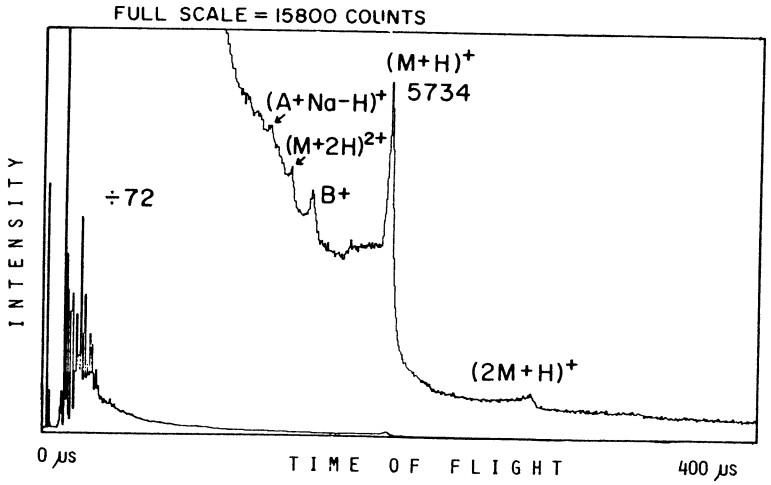

Fig. 3. Time-of-flight spectrum of bovine insulin with no metastable ion rejection. The mass range covered is 0–31 600 u.

TABLE 1

The measured isotopically averaged values of m/z for high mass peaks of bovine insulin compared with the calculated m/z values for the probable ion species observed

Probable ion species	Calculated [a] m/z	Measured m/z
$(A+Na-H)^+$	2359.6	2360.2 ± 2.0
B^+	3399.6	3398.4 ± 2.0
$(M+H)^+$	5734.7	5733.7 ± 2.0
$(M+2H)^{2+}$	2867.9	2864.2 ± 2.0
$(2M+H)^+$	11468	11463 ± 10

[a] Isotopically averaged mass.

observed (dimer, doubly charged QM ion, and A- and B-chain fragments) have been previously described by other workers [10,14–16]. The origin of the ion which we have designated $(A + Na - H)^+$ is puzzling because no significant $(M + Na)^+$ peak is observed in the spectrum. We note that a low intensity peak with a corresponding mass can be seen in the high resolution fast atom bombardment spectrum of insulin given in ref. 16.

A considerable intensity of low mass ions is also observed (see Fig. 3). Most of the structurally significant fragment ions identified below m/z 1000 appear to be related to the B-chain of insulin. These fragments will not be discussed in detail in the present paper.

A striking feature of the spectrum shown in Fig. 3 is the intense continuum of ions stretching from low to high masses. This continuum comprises the bulk of the ions observed above m/z 100 and will be discussed presently. For the purpose of peak identification, it is convenient to subtract this smooth continuum from the spectrum. The results of such a continuum subtraction is shown in Fig. 4 for the mass region between m/z 2000 and 40 000. In addition to the peaks already described, two higher mass peaks can be discerned which correspond in mass approximately to trimer and tetramer cluster ion species of insulin. To enhance the signal-to-noise ratio for these weak cluster ion peaks, the acceleration distance $d_{\text{foil-A}}$ (Fig. 2) was decreased to 1.5 mm and the run time increased to 1068 min for this run.

Close inspection of the structure centered at the protonated molecular ion peak reveals that it has a complex shape with at least three components.

(a) A small sharp roughly symmetrical component with a full width at half maximum (FWHM) of 125 ns, corresponding to a mass width of 8 u. This very narrow peak is too sharp to be apparent in the highly compressed representation of the spectrum given in Fig. 4. The measured width of 8 u is consistent with the width of the distribution of the isotopic components of

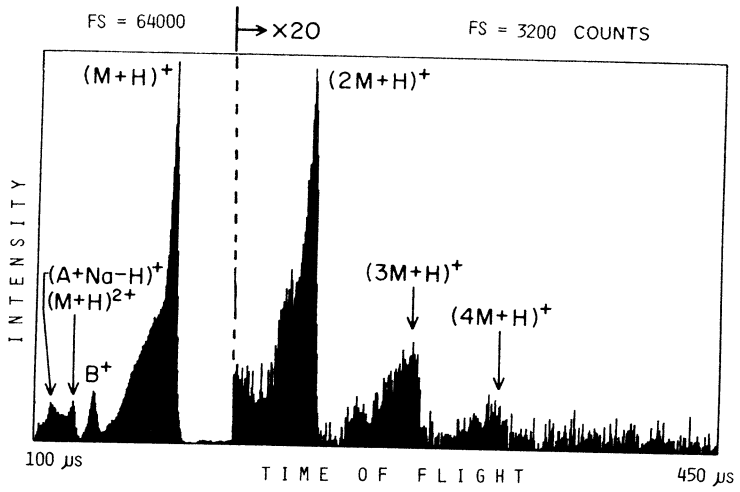

Fig. 4. Continuum subtracted time-of-flight spectrum of bovine insulin. The mass range covered is 2000–40000 u. The expected positions for the trimer and tetramer insulin ions are indicated.

insulin. Experiments described later in this section reveal that this sharp component is either stable over the full flight time or decays to fragment ions with a mass greater than 84% that of the precursor $(M + H)^+$ ion.

(b) A large broad roughly symmetrical component with a FWHM of 4000 ns which corresponds to a mass width of 271 u. At least some of this width can be attributed to broadening arising from the release of internal energy of excitation as fragment kinetic energy during metastable fragmentation of $(M + H)^+$ ions in the flight tube.

(c) A broad feature on the low time (mass) side of the $(M + H)^+$ peak extending some 1250 u below the sharp component. We attribute this feature to a series of unresolved fragment peaks resulting from losses of neutral molecules with masses up to 1250 u from the $(M + H)^+$ ion. Probable candidates for the fragmentations are the C-terminal 11 residues of the B-chain, the N-terminal 6 residues of the B-chain and the N-terminal 5 residues of the A-chain. All of these fragmentations involve the cleavage of just a single bond. Because of the intramolecular disulphide bridges, fragmentations of the molecular ion involving other parts of the molecule must occur through the rupture of at least two bonds and are thus less likely.

The results of two kinds of metastable fragmentation experiments are given.

Experiment 1. Flight-tube fragmentations integrated over 314 cm flight path

In this first experiment, we investigated the integrated metastable fragmentation of ions, formed from the insulin sample, throughout the whole

length of the 3 m long flight-tube, after acceleration to full energy. The sample foil was maintained at a potential of 10.1 kV and grids A, B, and C (see Fig. 2) at a potential of 0 V. Ions which decay in the field-free flight-tube give rise to fragments which have lower energies than their precursor ions [9,19]. By the application of appropriate potentials to grid E (Fig. 2), flight-tube metastable fragment ions may either be reflected and thus not detected or alternatively be separated from the precursor ions [9,19]. In previous work on chlorophyll *a* and smaller molecules [6,7,9], we were able to use such separated metastable fragment and precursor ion peaks to map detailed discrete fragmentation pathways. Due to the complexity of the present system, it was not practical to obtain analogous discrete fragmentation pathways. Here, metastable fragmentation distributions were mapped simply to different mass ranges. Thus, a series of potentials V_{DEC} was applied to grid E (Fig. 2) with magnitudes of 0.0, 2.0, 4.4, 6.5 and 8.5 kV. Ion fragments with

$$M(\text{fragment}) < (q_D V_{DEC}/q_A V_{ACC}) \times M(\text{precursor}) \quad (1)$$

where q_A is the charge on the accelerated ion, q_D is the charge on the decelerated ion, and V_{ACC} is the acceleration potential maintained at 10.1 kV, are reflected and are thus not detected. Data showing the effect on the spectrum of the application of these different potentials to grid E are given in Fig. 5. Clearly, both the peaks and the continuum get smaller as larger deceleration potentials are applied, corresponding to the rejection of increasing amounts of flight-tube fragmentation products. Measurements performed at elevated pressures demonstrated that collision-induced dissociation did not contribute significantly to the observed fragmentation.

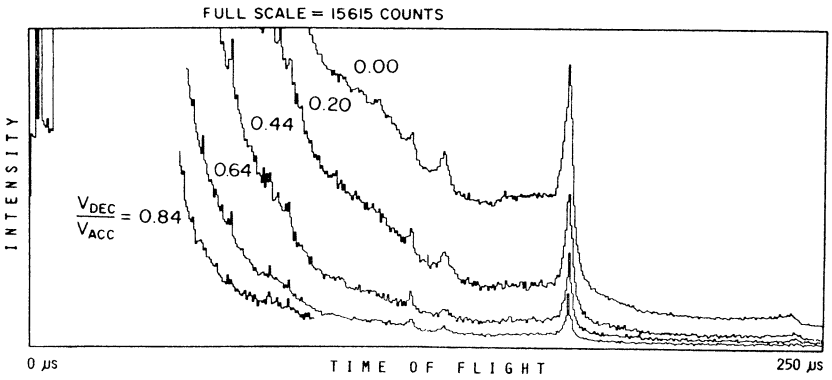

Fig. 5. Time-of-flight spectra of bovine insulin taken with five different magnitudes of the ratio of the deceleration potential to the acceleration potential, V_{DEC}/V_{ACC}. The run at 0.84 is only represented up to 90 μs for the sake of clarity.

TABLE 2

The percentage of ions which either do not fragment or which fragment to masses > $(q_D V_{DEC}/q_A V_{ACC}) \times M$(precursor) during their transit through the field-free flight-tube

Ion species	V_{DEC}/V_{ACC}				
	0.00	0.20	0.44	0.64	0.84
$(2M+H)^+$	100	64 ± 10	25 ± 5	< 4	< 4
$(M+H)^+$	100	55 ± 5	29 ± 6	13 ± 3	10 ± 3
B^+	100	75 ± 7	33 ± 10	19 ± 6	17 ± 6
$(M+2H)^{2+}$	100	81 ± 20 [a]	58 ± 16 [a]	47 ± 13 [a]	25 ± 8 [a]
$(A+Na-H)^+$	100	77 ± 28	38 ± 19	18 ± 9	15 ± 7

[a] Special consideration needed (see text).

Data showing the percentage of ions which do not fragment or which fragment to ions with masses > $(q_D V_{DEC}/q_A V_{ACC}) \times M$(precursor) during their transit through the flight tube are given in Table 2. The precursor ion species investigated were $(2M + H)^+$, $(M + H)^+$, $(M + 2H)^{2+}$, B^+ and $(A + Na - H)^+$. The indicated errors were estimated by comparing two completely independent duplicate experiments. Table 3 gives the time ranges over which the unimolecular fragmentations were measured. These limits correspond to the time after ion formation required for full acceleration of the ions and the flight time of ions to the retardation grid E.

It is important to note that the metastable fragmentation data reported in this paper do not represent absolute survival rates since the detection efficiency for ions of different masses is not known in the present experimental configuration. The data are, however, meaningful in operational terms and will be discussed as such. Inspection of Table 2 indicates that only a very small percentage (< 4%), if any, of the insulin dimer ions survive the 240 μs flight to the detector. Similarly, only 10% of the protonated molecular ions which are still intact after 381 ns survive the remaining 170 μs flight to

TABLE 3

The time required for the acceleration of selected ions into the field-free flight-tube and the flight time of these ions to the deceleration grid E (Fig. 2)

Ion species	Acceleration time (ns)	Flight time (μs)
$(2M+H)^+$	539	240
$(M+H)^+$	381	170
$(M+2H)^{2+}$	269	120
B^+	293	131
$(A+Na-H)^+$	244	109

the detector or decay to fragment ions with masses greater than 84% that of the $(M + H)^+$ ion. Fully 45% of $(M + H)^+$ ions decay in flight to fragment ions with $m/z < 1200$. A significant proportion of these low mass fragment ions are probably formed by sequential metastable decay processes [6,7,20]. Indeed, the data presented in Table 2 indicate that the A- and B-chain fragment ions exhibit a propensity to undergo unimolecular decompositions comparable with that of the $(M + H)^+$ ions.

The gas phase decomposition of the $(M + H)^+$ ion of bovine insulin has previously been studied using fast atom (several keV) bombardment of the compound in an α-monothioglycerol matrix using a reversed geometry double-focussing deflection mass spectrometer in its mass analyzed ion kinetic energy spectrum (MIKES) mode of operation [16]. The $(M + H)^+$ ion was found to decompose primarily to the B-chain fragment ion. We compare the present $(M + H)^+$ unimolecular fragmentation results with the results deduced from the MIKES spectra. Higher rates of decomposition are observed in the fission fragment experiment and the distribution of fragment ions is different and more heavily weighted to lower masses. Experimental differences which could account for these observed discrepancies include the facts that (1) the fission fragment experiment measures decompositions occurring more than two orders of magnitude earlier in time than the measurement in the fast atom experiment, (2) fission fragments have an energy four orders of magnitude higher than that of the fast atoms used, and (3) the fission fragment result was obtained on a solid insulin sample whilst the fast atom result was obtained on insulin dissolved in a liquid matrix.

Special consideration is needed for the interpretation of the doubly charged QM ion fragmentation data in Table 2. The doubly charged ions are accelerated to twice the energy of the singly charged species and are thus extracted into the field-free flight tube $\sim 30\%$ faster. Furthermore, the doubly charged ion may decay into either a doubly charged fragment and a neutral fragment or into two singly charged fragments. The latter alternative is considered to be more probable on general energetic grounds and also from examination of the metastable fragmentation data where the doubly charged QM ion appears to exhibit higher survival rates than the singly charged QM ion unless q_D/q_A in Eq. (1) is assumed equal to $1/2$.

Similar flight-tube metastable data were obtained for the ions comprising the broad spectral continuum and are given in Table 4. Inspection of the unretarded spectrum of insulin shown in Fig. 3 reveals that this continuum contains the bulk of the ions observed above m/z 100. The detailed origin of the continuum remains to be defined, although we have proposed previously [7,9] that at least part may be due to the summed effect of many overlapping broad peak tails. We have shown that such extended peak tails arise from fragmentation in the acceleration region. The general trend of the data in

TABLE 4

The percentage of continuum ions which either do not fragment or which fragment to masses $> (q_D V_{DEC}/q_A V_{ACC}) \times M$(precursor) during their transit through the field-free flight tube

The relative errors for these measurements are estimated to be less than 10%.

Mass range	V_{DEC}/V_{ACC}			
	0.00	0.20	0.40	0.64
0–500	100	98	94	86
500–1000	100	78	51	25
1000–2000	100	68	30	14
2000–3000	100	54	19	11
3000–4000	100	44	14	8
4000–6000	100	41	16	8

Table 4 demonstrates that the continuum ions show an increasing tendency for metastable fragmentation with an increase in mass. The data indicate that a large proportion of the fragment ions comprising the continuum still contain sufficient energy of excitation so that further decomposition reactions occur with high probability.

Experiment 2. Flight-tube fragmentation during first centimetre of flight path

To obtain information relating to the temporal distribution of fragmentations within the flight tube, a second experiment was designed to investigate the proportion of the fragmentations occurring after acceleration and during the first cm of the 314 cm long flight tube. The metastable rejection grid E was set to 0 V, i.e. no metastable rejection. The products of unimolecular fragmentation in the region between grids A and B were separated from their precursor ions using the method described in detail in ref. 7. Briefly, the separation is achieved with an intermediate field-free zone between grids A and B which is held at a potential elevated above ground. Thus the potentials utilized were 10.1 kV on the sample foil, 2.0 kV on grids A and B and 0.0 kV on grid C. The products of fragmentation reactions occurring in the field-free region between grids A and B have the same velocity as their precursor ions. However, since their masses differ from the precursor ion masses, the final acceleration step between grids B and C serve to give them velocities different from that of the precursor ions.

Neglecting the acceleration time, which is small, the total flight-times are

$$t_{\text{precursor}} = \left(\frac{M}{2eV_{ACC}} \right)^{1/2} L \qquad (2)$$

$$t_{\text{fragment}} = \left(M_f/^2 \left\{ \frac{M_f e(V_{ACC} - V_A)}{M} + eV_A \right\} \right)^{1/2} L \qquad (3)$$

where M is the precursor mass, M_f the fragment mass, L the flight path, V_{ACC} the acceleration potential (10.1 kV), and V_A the potential on grids A and B (2.0 kV). Thus separation of the fragmentation products and their parent ion species is effected. The results of this experiment are presented in Table 5 for the precursor ion species listed. The third column of Table 5 gives the percentage of ions which either do not fragment during flight through the region between grids A and B or which fragment in this region to ions with a fragment-to-precursor ratio greater than M_{LIM}(fragment)/M(precursor) as given in column 2. The limiting mass ratio, M_{LIM}(fragment)/M(precursor), is deduced from the minimum value of the time difference $t_{\text{precursor}} - t_{\text{fragment}}$, which can be experimentally determined. Special consideration is again needed for the $(M + 2H)^{2+}$ ion because it probably decays into two singly charged ions. For the doubly charged ion, the third column of Table 5 gives the percentage of ions which either do not fragment during flight through the region between grids A and B or which fragment in this region to ions with $0.60 > M$(fragment)/M(precursor) > 0.43.

The fraction of ions which disintegrate between grids A and B (which corresponds to the first cm of field-free flight in Experiment 1) can now be compared with the fraction of ions which disintegrate over the full flight path (314 cm). Comparison of the data in the final column of Table 2 with that in Table 5 clearly shows that flight-tube fragmentations are heavily weighted to favor early times, i.e. high rate constants. Presumably the ions are formed with a wide distribution of rate constants and the results suggest that the high values of the rate constants dominate.

TABLE 5

The percentage of ions which either do not fragment during flight through the region between grids A and B (Fig. 2) or which decompose in this region to ions with a fragment to precursor ratio grater than M_{LIM}(fragment)/M(precursor).

Ion species	M_{LIM}(fragment)/ M(precursor)	% Survival
$(2M+H)^+$	0.80	73 ± 11
$(M+H)^+$	0.77	70 ± 10
$(M+2H)^{2+}$	0.43–0.60 [a]	42 ± 6 [a]
B^+	0.78	82 ± 12
$(A+Na-H)^+$	0.79	39 ± 6

[a] Special consideration needed (see text).

ACKNOWLEDGEMENTS

This work was supported in part by the Division of Research Resources, NIH. We wish to thank Mr. Louis Grace for experimental assistance and Ms. Gladys Roberts for typing the manuscript.

REFERENCES

1 R.D. Macfarlane and D.F. Torgerson, Science, 191 (1976) 920.
2 R.D. Macfarlane, in G.R. Waller and O.C. Dermer (Eds.), Biochemical Applications of Mass Spectrometry, Suppl. Vol. 1, Wiley, New York, 1980, p. 1209.
3 B.T. Chait, W.C. Agosta and F.H. Field, Int. J. Mass Spectrom. Ion Phys., 39 (1981) 339.
4 B. Sundqvist, I. Kamensky, P. Hakansson, J. Kjellberg, M. Salehpour, S. Widdiyasekera, J. Fohlman, P.A. Peterson and P. Roepstorff, Biomed. Mass Spectrom., 11 (1984) 242.
5 B.T. Chait, B.F. Gisin and F.H. Field, J. Am. Chem. Soc., 104 (1982) 5157.
6 B.T. Chait and F.H. Field, J. Am. Chem. Soc., 104 (1982) 5519.
7 B.T. Chait and F.H. Field, J. Am. Chem. Soc., 106 (1984) 1931.
8 B.T. Chait, J. Shpungin and F.H. Field, Int. J. Mass Spectrom. Ion Processes, 58 (1984) 121.
9 B.T. Chait and F.H. Field, Int. J. Mass Spectrom. Ion Phys., 41 (1981) 17.
10 P. Hakansson, I. Kamensky, B. Sundqvist, J. Fohlman, P. Peterson, C.J. McNeal and R.D. Macfarlane, J. Am. Chem. Soc., 104 (1982) 2948.
11 B. Sundqvist, A. Hedin, P. Hakansson, I. Kamensky, J. Kjellberg, M. Salehpour, G. Sawe and S. Widdiyasekera, Int. J. Mass Spectrom. Ion Phys., 53 (1983) 167.
12 M. Barber, R.S. Bordoli, G.J. Elliot, R.D. Sedgwick, A.N. Tyler and B.N. Green, J. Chem. Soc. Chem. Commun., (1982) 936.
13 A. Dell and H.R. Morris, Biochem. Biophys. Res. Commun., 106 (1982) 1456.
14 C. Fenselau, J. Yergey and D. Heller, Int. J. Mass Spectrom. Ion Phys., 53 (1983) 5.
15 D.M. Desiderio and I. Katakuse, Biomed. Mass Spectrom., 11 (1984) 55.
16 M. Barber, R.S. Bordoli, G.J. Elliott, A.N. Tyler, J.C. Bill and B.N. Green, Biomed. Mass Spectrom., 11 (1984) 182.
17 R.D. Macfarlane and D.F. Torgerson, Int. J. Mass Spectrom. Ion Phys., 21 (1976) 81.
18 C.J. McNeal, R.D. Macfarlane and E.L. Thurston, Anal. Chem., 51 (1979) 2036.
19 W.W. Hunt, Jr., R.E. Huffman and K.E. McGee, Rev. Sci. Instrum., 35 (1964) 82.
20 B.T. Chait, Int. J. Mass Spectrom. Ion Phys., 53 (1983) 227.